Article
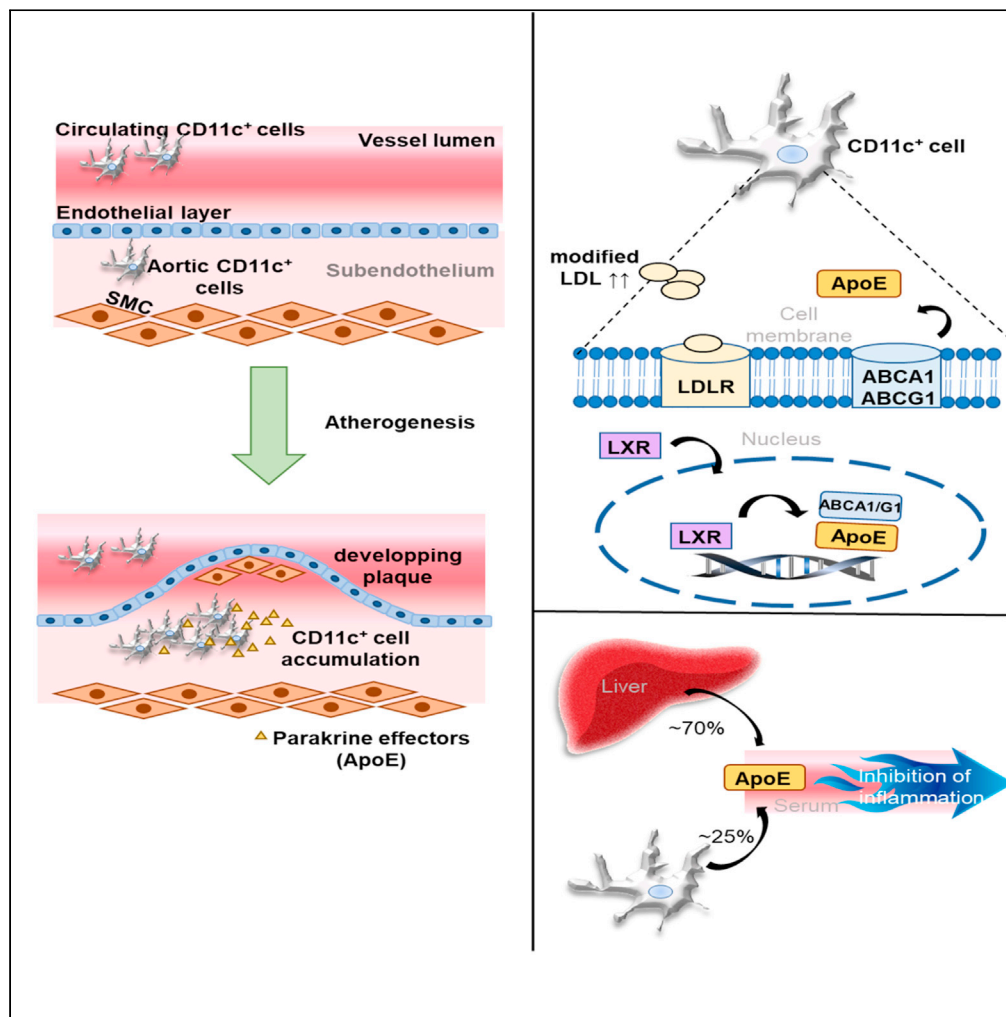
Apolipoprotein E derived from CD11c$^+$ cells ameliorates atherosclerosis

Manuela Sauter,
Reinhard J. Sauter,
Henry Nording, ...,
Sven Meuth,
Robert Feil, Harald
F. Langer

harald.langer@uksh.de

Highlights

CD11c$^+$ cells are enriched in aortae of high cholesterol-fed ApoE$^{-/-}$ mice

Depletion of CD11c$^+$ cells increases plaque size in ApoE$^{-/-}$ mice

≈ 20% of serum ApoE derives from CD11c$^+$ cells

ApoE from CD11c$^+$ cells contributes to protection from atherosclerosis

Article

Apolipoprotein E derived from CD11c⁺ cells ameliorates atherosclerosis

Manuela Sauter,[1,16] Reinhard J. Sauter,[1,16] Henry Nording,[1,2] Chaolan Lin,[1] Marcus Olbrich,[3] Stella Autenrieth,[4] Christian Gleissner,[5,17] Martin Thunemann,[6] Nadia Otero,[7] Esther Lutgens,[8] Zouhair Aherrahrou,[9] Dennis Wolf,[10] Lars Zender,[11,12,13] Sven Meuth,[14] Robert Feil,[15] and Harald F. Langer[1,18,*]

SUMMARY

Atherosclerosis is studied in models with dysfunctional lipid homeostasis—predominantly the ApoE$^{-/-}$ mouse. The role of antigen-presenting cells (APCs) for lipid homeostasis is not clear. Using a LacZ reporter mouse, we showed that CD11c⁺ cells were enriched in aortae of ApoE$^{-/-}$ mice. Systemic long-term depletion of CD11c⁺ cells in ApoE$^{-/-}$ mice resulted in significantly increased plaque formation associated with reduced serum ApoE levels. In CD11c^{cre+}ApoE$^{fl/fl}$ and Albumin^{cre+}ApoE$^{fl/fl}$ mice, we could show that $\approx$70% of ApoE is liver-derived and $\approx$25% originates from CD11c⁺ cells associated with significantly increased atherosclerotic plaque burden in both strains. Exposure to acLDL promoted cholesterol efflux from CD11c⁺ cells and cell-specific deletion of ApoE resulted in increased inflammation reflected by increased IL-1β serum levels. Our results determined for the first time the level of ApoE originating from CD11c⁺ cells and demonstrated that CD11c⁺ cells ameliorate atherosclerosis by the secretion of ApoE.

INTRODUCTION

Atherosclerosis still is the major cause of death in developed countries and accounts for an estimated 17.9 million deaths every year (WHO, 2019). A milestone for the elucidation of mechanisms contributing to atherosclerosis was the introduction of a mouse model for atherosclerosis, the ApoE$^{-/-}$ mouse (Zhang et al., 1992). Since the first experiments with this model, innumerable ApoE$^{-/-}$ mice have been analyzed in experiments worldwide. Surprisingly, however, the exact cellular source of ApoE has never been studied in detail. During atherogenesis, activation of immune processes and a sustained inflammatory reaction are major contributors to the pathogenesis of atherosclerosis (Libby et al., 2019, Wolf and Ley, 2019). An expansion of various immune cells such as T lymphocytes and macrophages, but also dendritic cells (DCs), has been demonstrated during atherosclerotic plaque growth (Tabas and Lichtman, 2017; Ait-Oufella et al., 2006; Wolf et al., 2015). While a significant body of evidence exists for the role of macrophages in atherosclerotic lesions, the function and relevance of DCs in this setting is not sufficiently characterized. It was, however, observed that the number of DCs and macrophages increases significantly during atheroprogression in the aortae of mice (Yilmaz et al., 2004; Cybulsky et al., 2016; Koltsova and Ley, 2011).

ApoE is a very well-studied gene, its product being a plasma glycoprotein of 34 kDa (Mahley et al., 2009). It has a protective role in atherosclerosis and is present in almost all serum lipoproteins. In humans, ApoE appears in three common alleles (ApoE*2, E*3, and E*4), which are more or less potent regulators of lipid metabolism based on their differences in receptor-binding activity and preference for lipoprotein association (Corder et al., 1993; Fan et al., 2007; Mahley et al., 2009; Weisgraber and Shinto, 1991). Data on its exact distribution, however, are not available. Particularly, the cell type of bone marrow-derived cells that is responsible for release of ApoE into the serum has not been thoroughly investigated, yet.

In this study, we characterized the cellular origin of ApoE *in vivo* and identified CD11c⁺ cells as relevant contributors to ApoE levels in the serum, thereby uncovering the important role of these cells for the prevention of atherogenesis.

[1]Department of Cardiology, University Hospital, Medical Clinic II, University Heart Center Luebeck, Ratzeburger Allee 160, 23538 Luebeck, Germany

[2]DZHK (German Research Centre for Cardiovascular Research), Partner Site Hamburg/Luebeck/Kiel, 23562 Luebeck, Germany

[3]University Hospital, Department of Cardiology, Eberhard Karls University Tuebingen, 72076 Tuebingen, Germany

[4]University Hospital, Department of Hematology and Oncology, Eberhard Karls University Tuebingen, 72076 Tuebingen, Germany

[5]University Hospital, Department of Cardiology, University of Heidelberg, 69120 Heidelberg, Germany

[6]Department of Biomedical Engineering, Boston University, Boston, MA 02215, USA

[7]Philipps University Marburg, Faculty of Medicine, 35043 Marburg, Germany

[8]University Hospital Munich, Institute for Prophylaxis and Epidemiology of Circulatory Diseases, Ludwig-Maximilians-University Munich, 80336 Munich, Germany

[9]University of Luebeck, Institute of Cardiogenetics, 23538 Luebeck, Germany

[10]University Hospital, Department of Cardiology and Angiology, University Heart Center Freiburg – Bad Krozingen, 79106 Freiburg, Germany

[11]Department of Medical Oncology and Pneumology (Internal Medicine VIII), University Hospital Tuebingen, 72076 Tuebingen, Germany

Continued

RESULTS

CD11c^{+} cells accumulated in developing atherosclerotic plaques, and depletion of these cells aggravated atherosclerosis

As a starting point, we analyzed the distribution of DCs (CD45^{+}/CD11c^{+}/MHCII^{+} cells) in murine aortae by flow cytometry. The gating strategy is depicted in Figure 1A. We found that CD11c^{+}/MHCII^{+} cells accumulate under atherosclerotic conditions in ApoE^{−/−} mice fed with high-cholesterol (HC) diet, as CD11c^{+}/MHCII^{+} cells were significantly increased in the aortae of atherosclerotic mice at HC diet for 12 weeks in comparison to C57Bl/6J (WT) mice of the same age fed a standard diet (Figure 1B). To be able to visualize antigen-presenting cells (APCs) in plaques of ApoE^{−/−} mice, we generated CD11c-reporter mice (Figure S1A). In these mice, β-galactosidase is expressed in all CD11c^{+} cells, which enables their detection and quantification (Figures 1C–1E). These mice were fed with standard or HC diet, and X-Gal staining was used to detect CD11c^{+} cells in cre-expressing mice. Figure 1D shows that CD11c^{+} cells accumulated on the surface of the plaques. Interestingly, upon feeding a HC diet, the presence of CD11c^{+} cells increased as atherosclerosis aggravated (Figures 1D and 1E).

Using a further *in vivo* approach for long-term depletion of CD11c^{+} cells, bone marrow from CD11c.DTR-GFP transgenic animals was transferred into ApoE^{−/−} mice (Figures S1B and S1C). After successful bone marrow engraftment, the HC diet was started and the mice were injected with diphtheria toxin twice weekly. Six weeks after DT treatment, the spleens were taken from the animals; single cell suspensions were prepared and analyzed for the presence of CD11c and GFP using flow cytometry. After 6 weeks depletion time, the sera of the bone marrow (BM) chimeras were screened for anti-DT antibodies, which were below the detection limit (Figure S1D). As shown in Figures S2A–S2E, we achieved an effective depletion of CD11c^{+} cells after six weeks in comparison to vehicle-treated chimeras. In order to investigate which DC cell type was depleted in the bone marrow chimeras, we analyzed the CD11c^{+} cells in single-cell suspensions of spleen cells for their surface markers. The number of CD11c[single+] cells was significantly reduced after six weeks of DT treatment (Figures S2A and S2B). Flow cytometric analysis moreover showed a significant depletion of GFP/CD11c double-positive cells in DT-treated BM chimeras. A further in-detail analysis revealed that although CD11c single-positive cells were significantly depleted, CD11c/CD11b double-positive cells were not, and that the depleted CD11c^{high} cell population were CD103 positive (FiguresS2A–S2E of the revised manuscript).

Furthermore, peripheral blood of the BM chimeras was screened for cell counts of white blood cells (wbc), red blood cells (rbc), and platelets (pltl), and no significant change in either of these cell types was observed (Figure S3A). To exclude that DT per se could have an impact on atheroprogression, we analyzed aortae of HC-fed ApoE^{−/−} mice treated with DT versus vehicle-treated animals and observed no significant differences in plaque areas (Figure S3B). In order to answer the question whether CD11c^{+} cells contribute to the progression of atherosclerosis or instead have an atheroprotective effect, the aortae of the chimeric atherosclerotic mice were explanted to quantify atheroprogression. We stained the aortae with Oil Red O and measured the plaque areas in relation to the total area (Figure 1F). Interestingly, the long-term depleted animals had a significantly larger plaque area compared with the non-depleted animals (Figure 1G). Furthermore, the lipid values in the sera of the animals were analyzed. In accordance with our previous results, total cholesterol and LDL cholesterol were significantly higher in the DT-treated animals (Figure 1H). Together, these data indicate that the distribution of CD11c^{+} cells in HC-fed ApoE^{−/−} mice differs significantly from that in WT mice, and that CD11c^{+} cells ameliorate atherosclerosis *in vivo*.

CD11c^{+} cells showed increased cholesterol efflux and secreted ApoE after exposure to acLDL

To determine which genes are regulated under atherosclerotic conditions, we performed affymetrix gene chip experiments with gene set enrichment analysis of CD11c^{+} immune cells from spleens of WT mice compared to CD11c^{+} cells isolated from spleens of ApoE^{−/−} mice on standard or HC diet, respectively. We found that genes belonging to the "immune-cell-signaling" pathway were significantly enriched in HC-fed compared to standard diet-fed mice (Figures S4A–S4C). Interestingly, we detected several direct or indirect interaction partners of ApoE such as PON1, LPL, Nf-κβ, SELE, and MSR1 (Gaidukov et al., 2010; Mullick et al., 2002; Li et al., 2011; Lahiri, 2004; Van Eck et al., 2000). Cholesterol efflux is the first step in reverse cholesterol export, which is mediated by a group of membrane transporters, including ATP-binding cassette transporter A1 and G1 (Gui et al., 2016). ApoE is primarily lipidated via ABCA1, and both are under transcriptional regulation by the nuclear liver X receptor (LXR) (Beyea et al., 2007). In BM-derived CD11c^{+} cells (Figure S5) exposed to an atherosclerotic environment *in vitro* (by adding acLDL to the

[12]DFG Cluster of Excellence 2180 'Image-guided and Functional Instructed Tumor Therapy' (IFIT), University of Tuebingen, 72076 Tuebingen, Germany

[13]German Cancer Research Consortium (DKTK), Partner Site Tübingen, German Cancer Research Center (DKFZ), 69120 Heidelberg, Germany

[14]University Hospital, Department of Neurology, University of Duesseldorf, 40225 Duesseldorf, Germany

[15]Interfaculty Institute of Biochemistry, University of Tuebingen, 72076 Tuebingen, Germany
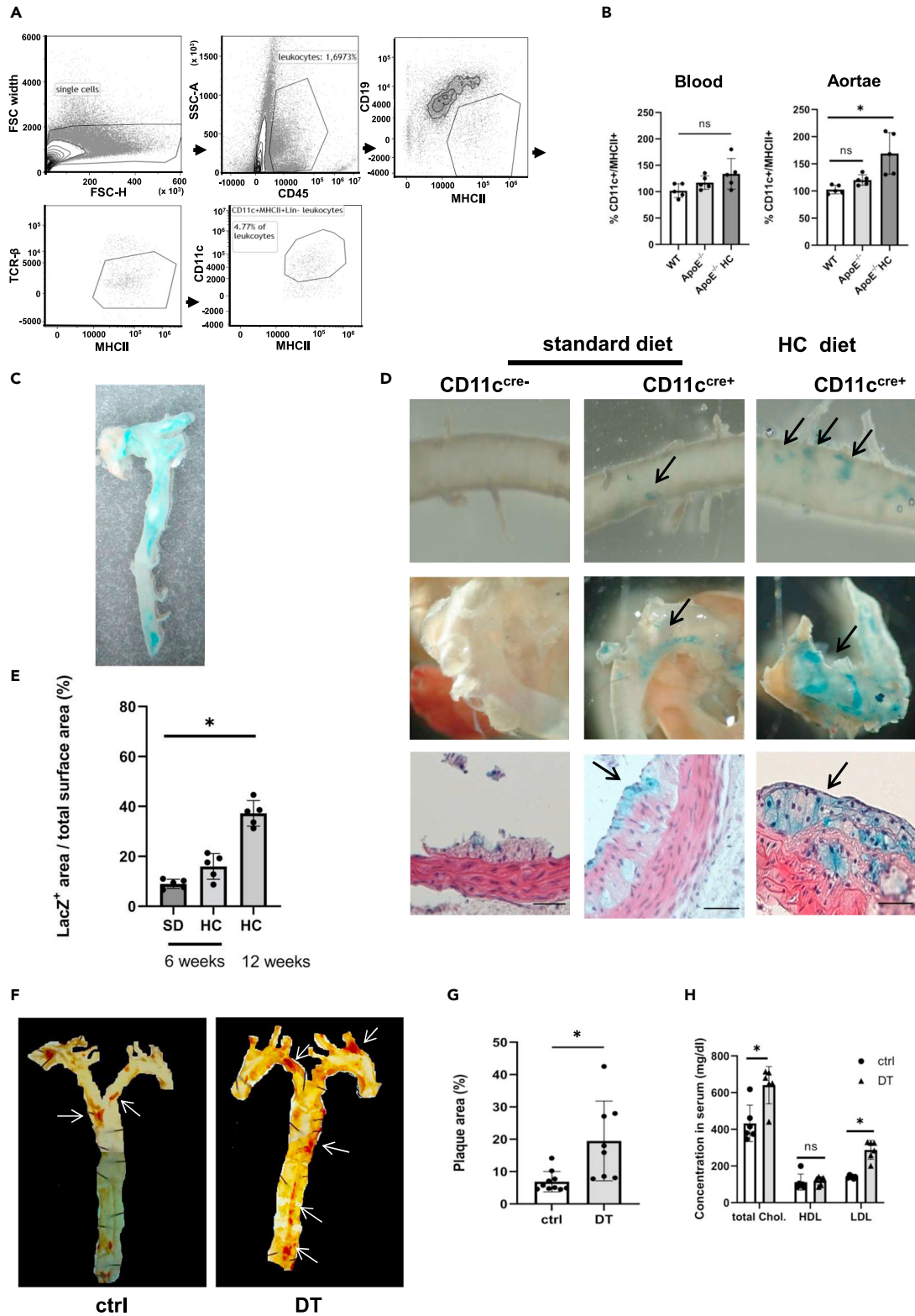
[16]These authors contributed equally

[17]Present address: Rottal-Inn Kliniken Eggenfelden, Department of Cardiology, 84307 Eggenfelden, Germany

[18]Lead contact

*Correspondence: harald.langer@uksh.de

https://doi.org/10.1016/j.isci.2021.103677

Figure 1. CD11c$^+$ cells accumulated in developing atherosclerotic plaques, and depletion of these cells aggravated atherosclerosis

(A) Detection and gating strategy of aortic CD11c$^+$ cells in WT mice.

(B) FACS analysis of CD11c$^+$/MHCII$^+$ double-positive cells in blood (left) and aortae (right) of ApoE$^{-/-}$ mice fed a high-cholesterol diet (HC) for a period of 12 weeks compared to standard diet-fed WT and ApoE$^{-/-}$ mice. During atheroprogression, we observed a significant accumulation of CD11c$^+$/MHCII$^+$ cells in aortae, but not in the peripheral blood. n = 5 animals per group. *p<0.05 vs WT mice.

(C) Using a CD11c reporter mouse approach (see also Figure S1A), morphometry of the blue signal allowed to analyze the area covered by CD11c$^+$ cells within the aorta.

(D and E) ApoE$^{-/-}$CD11c^{cre+}LacZ$^{fl/fl}$ mice were fed with standard or HC diet for a period of 6 or 12 weeks as indicated. Removed aortae were fixed with glutaraldehyde and PFA and stained with X-Gal. CD11c$^+$ cells that express LacZ could be visualized by their blue color macroscopically and microscopically (in sections of aortae, scale bar: 50μm). Images representative for 5 experiments were depicted. (E) Quantification showed a significant increase of CD11c$^+$ cells in the aortae during atherogenesis. n = 5 animals per group. *p<0.05.

(F and G) Evaluation of plaque development in a long-time depletion model for the ablation of CD11c$^+$ cells using bone marrow of CD11c$^+$-diphtheria toxin receptor (DTR)-GFP mice transferred into ApoE$^{-/-}$ mice. After depletion of CD11c$^+$ cells for 6 weeks, aortae were carefully perfused with PBS and fixed with 4% PFA, and dissected aortae were objected to Oil Red O staining. Plaque area was measured, and the quantification showed that plaque area in DT-treated BM chimeras was significantly increased in comparison to vehicle-ctrl-treated animals. n= 8–10 animals per group. *p<0.05 vs ctrl.

(H) Measurement of lipid parameters in sera of BM chimeras showed a significantly higher amount of total cholesterol and LDL cholesterol, whereas HDL levels remained unchanged. n = 6 animals per group. *p<0.05 vs. ctrl. Data are the mean ± SD.

medium), we were able to show that genes for LXR as well as its downstream targets ABCA1 and ABCG1 and ApoE itself (Figures 2A–2C) were upregulated. We furthermore compared BM-derived CD11c$^+$ cells from LXR knockout mice with WT BM-derived CD11c$^+$ cells using qPCR and observed that upon acLDL loading, LXR-knockout BM-derived CD11c$^+$ cells express significantly less ApoE (Figure 2D). To question the relevance of CD11c$^+$ cells for providing ApoE, BM-derived CD11c$^+$ cells were loaded with acLDL *in vitro*. 24 h after loading, the ApoE secretion into the culture supernatant was analyzed by western blotting. As shown in Figure 2E, a signal for ApoE protein was already detected in untreated cells, and in BM-derived CD11c$^+$ cells loaded with acLDL, the secretion was significantly increased. Using BM-derived CD11c$^+$ cells, we found that these cells, if exposed to an atherosclerotic environment (created by loading the cells with acLDL), show significantly increased cholesterol efflux compared to ctrl-loaded cells (Figure 2F).

CD11c$^+$ cell depletion reduced ApoE levels *in vivo* under pro-atherosclerotic conditions

To understand how acLDL affects signaling pathways of BM-derived CD11c$^+$ cells, we analyzed phosphorylation of intracellular signaling proteins. We found that exposition to the atherosclerotic stimulus *in vitro* upregulated most of the analyzed parameters, whereas phosphorylation of the serine-threonine kinase GSK-3β was not increased. We detected a particularly strong upregulation of signaling proteins functionally related to ApoE signaling such as STAT-1 (Trusca etal., 2011) (Figure 3A). The next step was to check the ApoE serum content *in vivo* using Western blot and ELISA of ApoE$^{-/-}$ mice reconstituted with bone marrow of CD11c.DTR-GFP mice. Interestingly, we found that depletion of CD11c$^+$ cells by DT treatment resulted in clearly reduced amounts of ApoE in the serum (Figures 3B and 3C). Together, CD11c$^+$ cells have a changed gene expression profile in atherosclerosis and secrete ApoE after acLDL loading *ex vivo* as well as under atherosclerotic conditions *in vivo*.

ApoE from CD11c$^+$ cells contributed with ∼20% to serum ApoE levels thereby lowering hypercholesterolemia, dampening vascular inflammation and protecting from atherosclerosis

In order to further characterize the relevance of ApoE derived from CD11c$^+$ cells, CD11c^{cre+} mice or Albumin^{cre+} mice were crossed with animals, in which the ApoE gene is "floxed". Using this approach, ApoE could be selectively switched off in CD11c$^+$ cells (CD11c^{cre+}ApoE$^{fl/fl}$) or in albumin-expressing (Alb^{cre+}ApoE$^{fl/fl}$) liver cells (Figure 4A). Figures 4B and 4C shows by Western blot (Figure 4B) and ELISA (Figure 4C) that in CD11c$^+$-specific ApoE knockout mice, the ApoE serum levels were reduced by about 25% compared to WT animals, whereas in liver-specific ApoE knockout mice the ApoE content was obviously even more reduced. The animals were fed a HC diet for a period of 12 weeks and then the explanted aortae were stained with Oil Red O to visualize and quantify developing atherosclerotic plaques. We detected a clear and significant difference between Alb^{cre+}ApoE$^{fl/fl}$ and Alb^{cre-}ApoE$^{fl/fl}$ animals (Figure 4D). Furthermore, we observed that the plaque area was significantly larger in animals that are deficient for ApoE in CD11c$^+$ cells in comparison to CD11c^{cre-} control animals (Figure 4E). Compared to complete ApoE knockout mice, liver-specific ApoE$^{-/-}$ mice and DC-specific ApoE$^{-/-}$ mice had a smaller plaque area (Figures 4D and 4E). These data demonstrate that CD11c$^+$-derived ApoE contributes significantly to protection
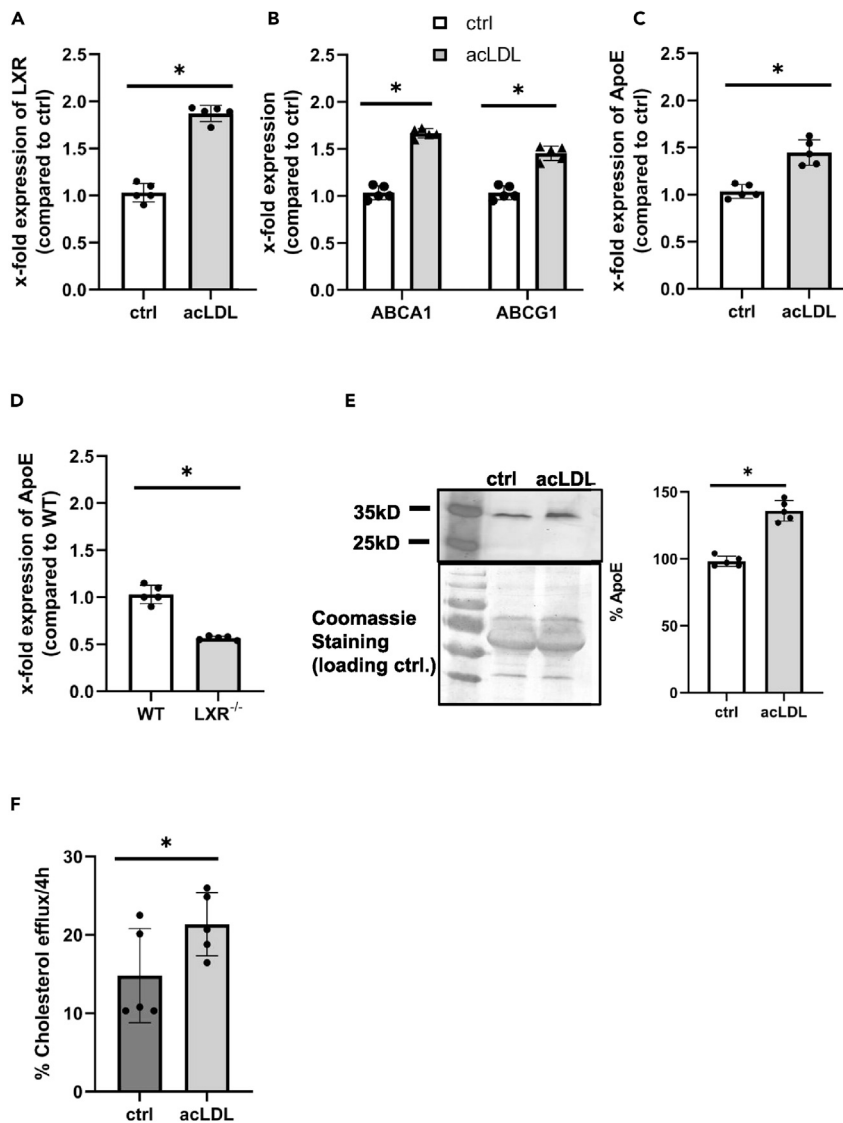
Figure 2. CD11c⁺ cells showed increased cholesterol efflux and were able to secrete ApoE after exposure to acLDL

(A–C) BM-derived CD11c⁺ cells were screened for expression of different genes relevant for cholesterol export using qPCR. n = 5 per group. *p<0.05 vs ctrl. In WT BM-derived CD11c⁺ cells, LXR was significantly upregulated upon treatment with acLDL (A) as well as its downstream targets ABCA1 and ABCG1 (B) and ApoE itself (C).

(D) In BM-derived CD11c⁺ cells isolated from LXR⁻/⁻ mice, ApoE mRNA was significantly reduced compared with WT BM-derived CD11c⁺ cells.

(E) BM-derived CD11c⁺ cells of WT mice were screened on day 7 of culture for their ability to secrete ApoE upon loading with acLDL. Culture supernatant was objected to western blotting 24 h after treatment with acLDL and screened for ApoE. AcLDL-treated BM-derived CD11c⁺ cells showed significantly increased levels of secreted ApoE. Blots were quantified by densitometry. n = 5, *p<0.05.

(F) Cholesterol efflux analysis of BM-derived CD11c⁺ cells revealed that cholesterol efflux was significantly enhanced if these cells were exposed to an atherosclerotic environment (loading with acLDL). (C–F) Data are the mean ± SD.

from atherosclerosis and that the amount of ApoE derived from CD11c⁺ cells makes up to 25% of total serum ApoE, whereas for liver-derived ApoE the proportion is around 70%.

To analyze systemic inflammation, we measured IL-1β levels in sera of CD11c^cre+ApoE^fl/fl mice (and Albumin^cre+ApoE^fl/fl mice as positive control) by ELISA and found that IL-1β levels were significantly
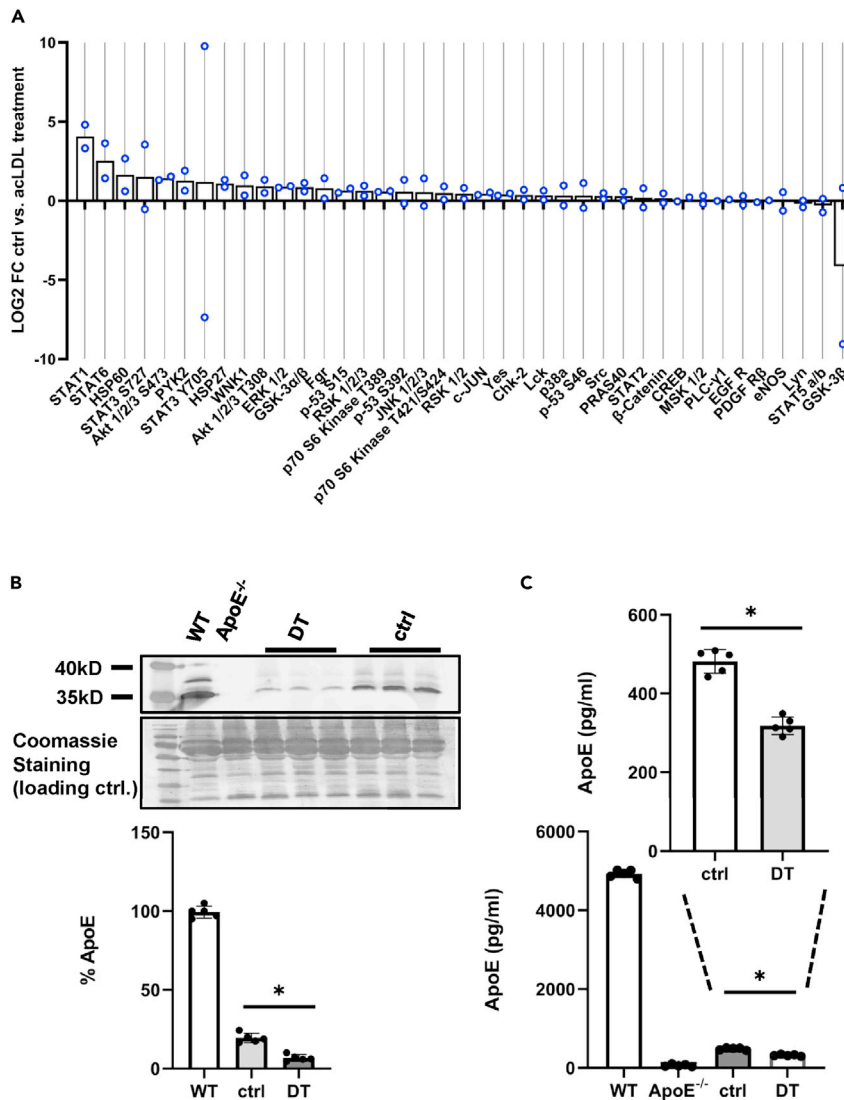
**Figure 3. CD11c+ cell depletion reduced ApoE levels *in vivo* under pro-atherosclerotic conditions**

(A) A phosphokinase antibody array was performed for analyzing lysates from BM-derived CD11c+ cells loaded with acLDL or vehicle control (ctrl) for 24h. Changes in phosphorylation were plotted as log2 fold change (FC) (n = 2 independent experiments).

(B and C) Sera of BM chimeras (DT-treated chimeras versus vehicle-treated (ctrl) chimeras) were analyzed for ApoE levels after a depletion period of 6 weeks by (B) Western Blot and (C) ELISA. ApoE$^{-/-}$ mice reconstituted with WT BM showed about ≈25% ApoE in serum compared with WT mice, whereas in DT-treated BM chimeras the increase in ApoE levels was significantly abolished. n = 5 animals per group. *p<0.05. Data are the mean ± SD.

enhanced after cell-specific knockdown in both CD11c+ cells and liver cells compared to cre-negative animals (Figure 4F), which indicates DC-specific prevention from inflammatory processes. These data underscore the role of CD11c+ cell-derived ApoE for atherosclerosis.

DISCUSSION

Antigen-presenting CD11c+ cells are present within the vessel wall and could be of functional relevance for vascular homeostasis (Yilmaz et al., 2004). CD11c, as well as MHC-II, is a well-established marker for APC and CD11c+/MHC-II^{high} cells are recognized as aortic DCs (Butcher and Galkina, 2012). However, CD11c expression is not limited to DCs exclusively but is also present on other cell types (Hou et al., 2020; Satpathy et al., 2012; Zernecke, 2015). More recently, the cellular network, which is formed by CD11c+ cells within the
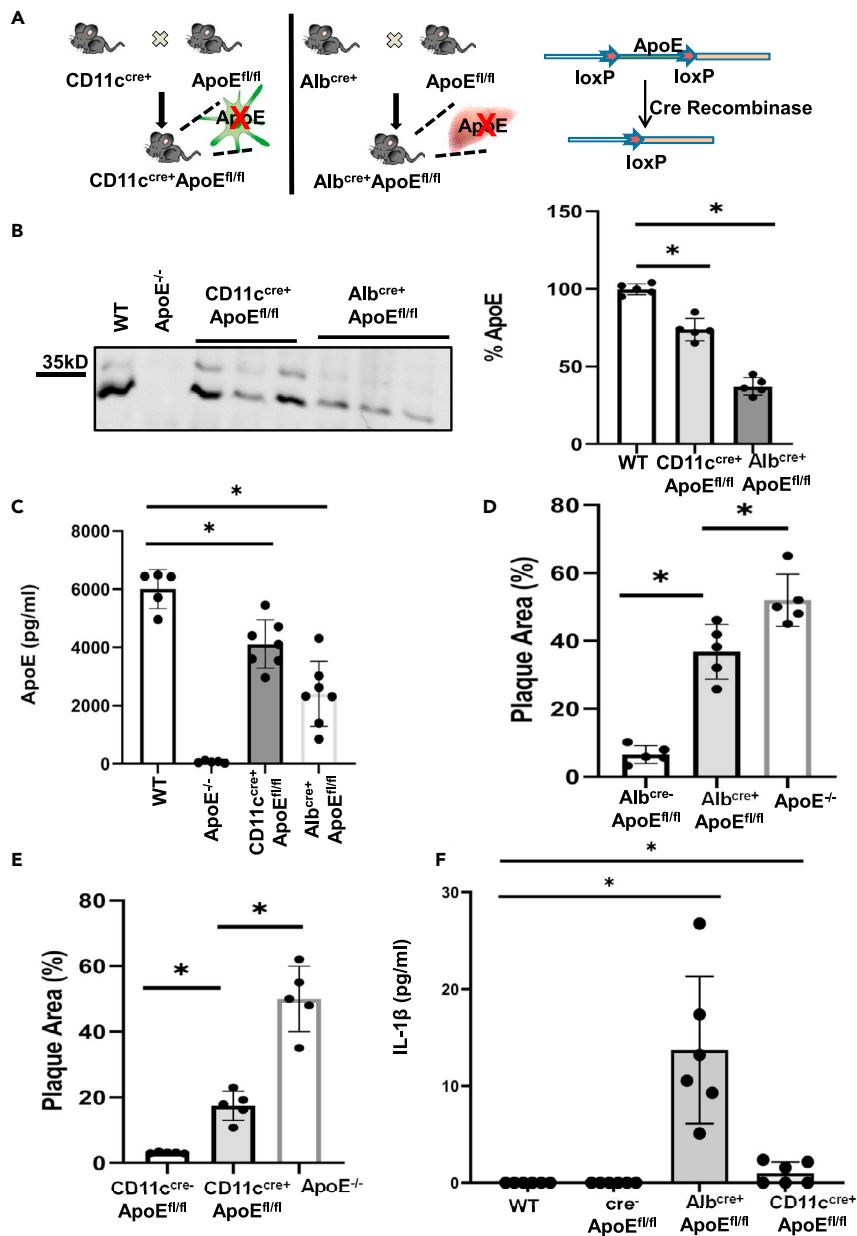
Figure 4. Generation and analysis of cell-specific ApoE knockout mice *in vivo*

(A) Cell-specific ApoE$^{-/-}$ mice were generated using the cre/lox system. For CD11c$^+$-specific knockout mice, ApoE$^{fl/fl}$ mice were bred to CD11c^{cre+} mice. For obtaining mice with liver-knocked out ApoE, Albumin^{cre+} mice were bred to ApoE$^{fl/fl}$ mice.

(Band C) Western blot (n = 5 animals per group. *p<0.05.) and (C) ELISA (n = 5–7 animals per group. *p<0.05.) analysis of sera for ApoE showed that ApoE levels in CD11c^{cre+}ApoE$^{fl/fl}$ mice were reduced by about 25%, whereas in Alb^{cre+}ApoE$^{fl/fl}$ mice we observed an even more pronounced and significant reduction of ApoE reflecting the bulk ApoE production in the liver.

(D and E) CD11c^{cre+}ApoE$^{fl/fl}$, Alb^{cre+}ApoE$^{fl/fl}$, and ApoE$^{-/-}$ mice were fed with HC diet for a period of 12 weeks and aortae were perfused with PBS, fixed with 4%PFA and dissected vessels, free from adventitia and surrounding fat tissue, were stained with Oil Red O. (D) Plaque area was measured and the analysis showed significantly reduced plaque development in Alb^{cre+}ApoE$^{fl/fl}$ compared with ApoE$^{-/-}$ mice. n = 5 animals per group. *p<0.05. (E) In CD11c^{cre+}ApoE$^{fl/fl}$mice, plaque

Figure 4. Continued

development was significantly increased compared to cre⁻ littermates. ApoE⁻/⁻ mice served as positive ctrl. n = 5 animals per group. *p<0.05.

(F) IL-1β levels in sera of CD11c^{cre+}ApoE^{fl/fl} and Albumin^{cre+}ApoE^{fl/fl} were analyzed by ELISA. IL-1β levels appeared significantly enhanced after cell-specific knockdown in both CD11c⁺ and liver cells compared to cre⁻ animals. Data are the mean ± SD.

vascular wall, was visualized by the group of Ralph Steinman using a CD11c-YFP *in vivo* approach (Choi et al., 2009). Conflicting data on how CD11c⁺ cells affect atherosclerosis have been published. For instance, a transgenic approach with BcL-2 expression under a CD11c promoter causing *in vivo* expansion of DCs showed reduction of atherosclerosis (Gautier et al., 2009). This was in line with a further study, which demonstrated that Flt3 signaling-dependent DCs (defined as CD11c⁺MHCII⁺ cells) protect against athero-sclerosis (Choi et al., 2011). Another study, however, suggested that *in vivo* depletion of DCs using the CD11c-diphtheria toxin receptor model inhibits atherosclerosis (Paulson et al., 2010). Our observations were in line with the former study (Gautier et al., 2009), as long-term depletion of CD11c⁺ cells resulted in significantly increased atherosclerosis. It has to be mentioned, however, that the work by Paulson et al. was carried out using a short-term DC depletion approach, while we established a protocol, which makes it possible to deplete CD11c⁺ cells over a longer period of time to study their role in atherosclerosis. The atheroprotective role of ApoE is undebated, and the ApoE knockout model has served many researchers to understand the pathophysiology of atherosclerosis. Studies from years back assign the pro-duction of ApoE predominantly to the liver (Linton et al., 1991). Furthermore, a relevance of bone-marrow-derived cell (BMDC)-ApoE has been suggested before, as it can protect against atherosclerosis during both early (Bellosta et al., 1995) and late plaque development (Linton et al., 1995). This fact may explain our observation using the bone marrow transfer approach of CD11c.DTR⁺ cells, that apparently small dif-ferences in ApoE are sufficient to cause rather substantial changes in plaque area. Indeed, it was demon-strated that BMDC-derived ApoE can protect from atherosclerosis even in the absence of changes in serum lipid levels (Fazio et al., 2002). Furthermore, BMDC ApoE expression can alter lesion cell composition by modifying the recruitment of inflammatory Ly6C/CCR2⁺ monocytes (Murphy et al., 2011; Wang et al., 2014). Together with our data, this indicate that ApoE from cells of hematopoietic origin may have immu-nomodulatory functions, regardless of the onset of hypercholesterolemia, as our transcriptional analysis of mRNA isolated from isolated CD11c⁺ cells from spleens of ApoE⁻/⁻ and WT mice demonstrates an enrich-ment of genes important for immune cell signaling pathways. Bonacina et al. showed recently that ApoE deficiency leads to the accumulation of cholesterol in the cell membrane of DCs, resulting in enhanced MHC-II-dependent antigen presentation and CD4⁺T cell activation (Bonacina et al., 2018). We observed that genes relevant for cholesterol efflux in BM-derived CD11c⁺ cells were significantly altered in cells exposed to an atherosclerotic environment *in vitro* and we found that BM-derived CD11c⁺ cells exposed to an atherosclerotic environment show significantly increased cholesterol efflux compared to ctrl-loaded cell preparations. This could implicate that CD11c⁺ cells are at least partially responsible for reduced cholesterol accumulation within the plaque. Thus, this observation may represent one potential mecha-nism, how DCs reduce experimental atherosclerosis. To further investigate the effect of ApoE from CD11c⁺ cells, we generated cell-specific ApoE knockout mice deficient for ApoE in all CD11c⁺ cells, as well as liver-specific ApoE knockout mice (deficient for ApoE in all albumin-expressing cells). Interestingly, the CD11c^{cre+}ApoE^{fl/fl} animals showed increased plaque development, although the effect was not as strong as in liver-specific ApoE knockout mice. Our data derived from these genetic mouse models demon-strated to the best of our knowledge for the first time *in vivo* that the ApoE content *in vivo* stems to ≈70% from the liver and to ≈25% from BM-derived CD11c⁺ cells.

Interestingly, activation of the inflammasome was recently shown to link cellular cholesterol accumulation in DCs to acquired immunity (Westerterp et al., 2017). Furthermore, activation of the inflammasome in conventional DCs adversely affects the adaptive immune system (by disabling cDCs to activate both CD4⁺ and CD8⁺ T cells) and, thus, the disease process in atherosclerosis (McDaniel et al., 2020). Addi-tionally, it has been shown in murine macrophages that ApoE is capable of inhibiting activation of T cells (Tenger and Zhou, 2003). We found that ApoE deficiency in CD11c⁺ cells results in increased levels of IL-1β within the circulation consistent with increased atherosclerosis compared to cre-negative and WT mice. This, in our opinion, further underlines the potential interplay between metabolism and increased immune activation.

In summary, we demonstrated that CD11c^{+} cells secrete ApoE, which contributed significantly to protection from atherosclerosis and, thus, identified a novel intersection point between innate immunity and metabolism.

Limitations of the study

Our study certainly has several limitations. When speaking of CD11c^{+} cells as DCs, it has to be mentioned that the clear identification of DCs is complex, particularly as they have overlapping phenotypes and share surface receptors with other immune cells. Therefore, future studies will have to scrutinize the observed mechanisms in subtypes of CD11c^{+} cells. Importantly, data derived from bone marrow chimeric mice have to be interpreted carefully (Ferreira et al., 2019) as it has been shown that the bone marrow also contributes to Kupffer cell replenishment (Gale et al., 1978). Moreover, the distribution of ApoE among lipoprotein subclasses and even within the liver should be characterized, as they could serve as a source of local enrichment of hepatocyte cell surfaces to accentuate lipoprotein clearance. Future studies will furthermore have to investigate how the loss of ApoE in CD11c^{+} cells directly affects T cell priming.

STAR★METHODS

Detailed methods are provided in the online version of this paper and include the following:

- KEY RESOURCES TABLE
- RESOURCE AVAILABILITY
  - ○ Lead contact
  - ○ Materials availability
  - ○ Data and code availability
- EXPERIMENTAL MODEL AND SUBJECT DETAILS
  - ○ Mouse models
- METHOD DETAILS
  - ○ Isolation and cultivation of BM derived CD11c^{+} cells
  - ○ Generation of CD11c reporter mice
  - ○ Generation of cell-specific ApoE^{-/-} mice
  - ○ LacZ staining
  - ○ Generation of BM chimeras
  - ○ Oil red O staining
  - ○ Enzyme linked immunosorbent assay (ELISA)
  - ○ Proteome profiler
  - ○ Cholesterol efflux analysis
  - ○ Lipid analysis
  - ○ Flow cytometry
  - ○ Quantitative PCR
  - ○ Gene arrays
  - ○ Local pooled error test
  - ○ Gene set enrichment analysis
  - ○ Western Blot
- QUANTIFICATION AND STATISTICAL ANALYSIS
- ADDITIONAL RESOURCES

SUPPLEMENTAL INFORMATION

Supplemental information can be found online at https://doi.org/10.1016/j.isci.2021.103677.

REFERENCES

Ait-Oufella, H., Salomon, B.L., Potteaux, S., Robertson, A.-K.L., Gourdy, P., Zoll, J., Merval, R., Esposito, B., Cohen, J.L., Fisson, S., et al. (2006). Natural regulatory T cells control the development of atherosclerosis in mice. Nat. Med. *12*, 178–180.

Bellosta, S., Mahley, R.W., Sanan, D.A., Murata, J., Newland, D.L., Taylor, J.M., and Pitas, R.E. (1995). Macrophage-specific expression of human apolipoprotein E reduces atherosclerosis in hypercholesterolemic apolipoprotein E-null mice. J. Clin.Invest. *96*, 2170–2179.

Beyea, M.M., Heslop, C.L., Sawyez, C.G., Edwards, J.Y., Markle, J.G., Hegele, R.A., and Huff, M.W. (2007). Selective up-regulation of LXR-regulated genes ABCA1, ABCG1, and APOE in macrophages through increased endogenous synthesis of 24(S),25-epoxycholesterol. J. Biol. Chem. *282*, 5207–5216.

Bonacina, F., Coe, D., Wang, G., Longhi, M.P., Baragetti, A., Moregola, A., Garlaschelli, K., Uboldi, P., Pellegatta, F., Grigore, L., et al. (2018). Myeloid apolipoprotein E controls dendritic cell antigen presentation and T cell activation. Nat. Commun. *9*, 3083.

Buch, T., Heppner, F.L., Tertilt, C., Heinen, T.J., Kremer, M., Wunderlich, F.T., Jung, S., and Waisman, A. (2005). A Cre-inducible diphtheria toxin receptor mediates cell lineage ablation after toxin administration. Nat. Methods. *2*, 419–426.

Butcher, M.J., and Galkina, E.V. (2012). Phenotypic and functional heterogeneity of macrophages and dendritic cell subsets in the healthy and atherosclerosis-prone aorta. Front. Physiol. *3*, 44.

Cho, H.J., Shashkin, P., Gleissner, C.A., Dunson, D., Jain, N., Lee, J.K., Miller, Y., and Ley, K. (2007). Induction of dendritic cell-like phenotype in macrophages during foam cell formation. Physiol. Genomics. *29*, 149–160.

Choi, J.-H., Do, Y., Cheong, C., Koh, H., Boscardin, S.B., OH, Y.-S., Bozzacco, L., Trumpfheller, C., Park, C.G., and Steinman, R.M. (2009). Identification of antigen-presenting dendritic cells in mouse aorta and cardiac valves. J. Exp. Med. *206*, 497–505.

Choi, J.H., Cheong, C., Dandamudi, D.B., Park, C.G., Rodriguez, A., Mehandru, S., Velinzon, K., Jung, I.H., Yoo, J.Y., Oh, G.T., and Steinman, R.M. (2011). Flt3 signaling-dependent dendritic cells protect against atherosclerosis. Immunity *35*, 819–831.

Corder, E.H., Saunders, A.M., Strittmatter, W.J., Schmechel, D.E., Gaskell, P.C., Small, G.W., Roses, A.D., Haines, J.L., and Pericak-Vance, M.A. (1993). Gene dose of apolipoprotein E type 4 allele and the risk of Alzheimer's disease in late onset families. Science *261*, 921–923.

Cybulsky, M.I., Cheong, C., and Robbins, C.S. (2016). Macrophages and dendritic cells. Circ. Res. *118*, 637–652.

Fan, D., Qiu, S., Overton, C.D., Yancey, P.G., Swift, L.L., Jerome, W.G., Linton, M.F., and Fazio, S. (2007). Impaired secretion of apolipoprotein E2 from macrophages. J. Biol. Chem. *282*, 13746–13753.

Fazio, S., Babaev, V.R., Burleigh, M.E., Major, A.S., Hasty, A.H., and Linton, M.F. (2002). Physiological expression of macrophage apoE in the artery wall reduces atherosclerosis in severely hyperlipidemic mice. J. Lipid Res. *43*, 1602–1609.

Feil, S., Fehrenbacher, B., Lukowski, R., Essmann, F., Schulze-Osthoff, K., Schaller, M., and Feil, R. (2014a). Transdifferentiation of vascular smooth muscle cells to macrophage-like cells during atherogenesis. Circ. Res. *115*, 662–667.

Feil, S., Krauss, J., Thunemann, M., and Feil, R. (2014b). Genetic inducible fate mapping in adult mice using tamoxifen-dependent Cre recombinases. Methods Mol. Biol. 1215–5_6.

Ferreira, F.M., Palle, P., Vom Berg, J., Prajwal, P., Laman, J.D., and Buch, T. (2019). Bone marrow chimeras-a vital tool in basic and translational research. J. Mol. Med. *97*, 889–896.

Gaidukov, L., Viji, R.I., Yacobson, S., Rosenblat, M., Aviram, M., and Tawfik, D.S. (2010). ApoE induces serum Paraoxonase PON1 activity and stability similar to ApoA-I. Biochemistry *49*, 532–538.

Gale, R.P., Sparkes, R.S., and Golde, D.W. (1978). Bone marrow origin of hepatic macrophages (Kupffer cells) in humans. Science *201*, 937–938.

Gautier, E.L., Huby, T., Saint-Charles, F., Ouzilleau, B., Pirault, J., Deswaerte, V., Ginhoux, F., Miller, E.R., Witztum, J.L., Chapman, M.J., and Lesnik, P. (2009). Conventional dendritic cells at the crossroads between immunity and cholesterol homeostasis in atherosclerosis. Circulation *119*, 2367–2375.

Gui, Y.-Z., Yan, H., Gao, F., Xi, C., Li, H.-H., and Wang, Y.-P. (2016). Betulin attenuates atherosclerosis in apoE−/− mice by up-regulating ABCA1 and ABCG1. Acta Pharmacol. Sin. *37*, 1337–1348.

Hou, L., Voit, R.A., Sankaran, V.G., Springer, T.A., and Yuki, K. (2020). CD11c regulates hematopoietic stem and progenitor cells under stress. Blood Adv. *4*, 6086–6097.

Inaba, K., Inaba, M., Romani, N., Aya, H., Deguchi, M., Ikehara, S., Muramatsu, S., and Steinman, R.M. (1992). Generation of large numbers of dendritic cells from mouse bone marrow cultures supplemented with granulocyte/macrophage colony-stimulating factor. J. Exp. Med. *176*, 1693–1702.

Jain, N., Cho, H., O'connell, M., and Lee, J.K. (2005). Rank-invariant resampling based estimation of false discovery rate for analysis of small sample microarray data. BMC Bioinformatics *6*, 1471–2105.

Jain, N., Thatte, J., Braciale, T., Ley, K., O'connell, M., and Lee, J.K. (2003). Local-pooled-error test for identifying differentially expressed genes with a small number of replicated microarrays. Bioinformatics *19*, 1945–1951.

Jung, S., Unutmaz, D., Wong, P., Sano, G.-I., de Los Santos, K., Sparwasser, T., Wu, S., Vuthoori, S., Ko, K., Zavala, F., et al. (2002). In vivo depletion of CD11c+ dendritic cells abrogates priming of CD8+ T cells by exogenous cell-associated antigens. Immunity *17*, 211–220.

Koltsova, E.K., and Ley, K. (2011). How dendritic cells shape atherosclerosis. Trends Immunology *32*, 540–547.

Lahiri, D.K. (2004). Apolipoprotein E as a target for developing new therapeutics for Alzheimer's disease based on studies from protein, RNA, and regulatory region of the gene. J. Mol. Neurosci. *23*, 225–233.

Langer, H.F., Choi, E.Y., Zhou, H., Schleicher, R., Chung, K.J., Tang, Z., Gobel, K., Bdeir, K., Chatzigeorgiou, A., Wong, C., et al. (2012). Platelets contribute to the pathogenesis of experimental autoimmune encephalomyelitis. Circ. Res. 110, 1202–1210.

Li, X., Johnson, K.R., Bryant, M., Elkahloun, A.G., Amar, M., Remaley, A.T., De Silva, R., Hallenbeck, J.M., and Quandt, J.A. (2011). Intranasal delivery of E-selectin reduces atherosclerosis in ApoE-/- mice. PLoS One 6, e20620.

Libby, P., Buring, J.E., Badimon, L., Hansson, G.K., Deanfield, J., Bittencourt, M.S., Tokgözoğlu, L., and Lewis, E.F. (2019). Atherosclerosis. Nat. Rev. Dis. Primers 5, 56.

Linton, M.F., Atkinson, J.B., and Fazio, S. (1995). Prevention of atherosclerosis in apolipoprotein E-deficient mice by bone marrow transplantation. Science 267, 1034–1037.

Linton, M.F., Gish, R., Hubl, S.T., Butler, E., Esquivel, C., Bry, W.I., Boyles, J.K., Wardell, M.R., and Young, S.G. (1991). Phenotypes of apolipoprotein B and apolipoprotein E after liver transplantation. J. Clin.Invest. 88, 270–281.

Mahley, R.W., Weisgraber, K.H., and Huang, Y. (2009). Apolipoprotein E: structure determines function, from atherosclerosis to Alzheimer's disease to AIDS. J. Lipid Res. 50, 22.

McDaniel, M.M., Kottyan, L.C., Singh, H., and Pasare, C. (2020). Suppression of inflammasome activation by IRF8 and IRF4 in cDCs is critical for T cell priming. Cell Rep. 31, 107604.

Muller, I., Schonberger, T., Schneider, M., Borst, O., Ziegler, M., Seizer, P., Leder, C., Muller, K., Lang, M., Appenzeller, F., et al. (2013). Gremlin-1 is an inhibitor of macrophage migration inhibitory factor and attenuates atherosclerotic plaque growth in ApoE-/- Mice. J. Biol. Chem. 288, 31635–31645.

Mullick, A.E., Deckelbaum, R.J., Goldberg, I.J., Al-Haideri, M., and Rutledge, J.C. (2002). Apolipoprotein E and lipoprotein lipase increase triglyceride-rich particle binding but decrease particle penetration in arterial wall. Arteriosclerosis Thromb.Vasc. Biol. 22, 2080–2085.

Murphy, A.J., Akhtari, M., Tolani, S., Pagler, T., Bijl, N., Kuo, C.L., Wang, M., Sanson, M., Abramowicz, S., Welch, C., et al. (2011). ApoE regulates hematopoietic stem cell proliferation, monocytosis, and monocyte accumulation in atherosclerotic lesions in mice. J. Clin.Invest. 121, 4138–4149.

Paulson, K.E., Zhu, S.N., Chen, M., Nurmohamed, S., Jongstra-Bilen, J., and Cybulsky, M.I. (2010). Resident intimal dendritic cells accumulate lipid and contribute to the initiation of atherosclerosis. Circ. Res. 106, 383–390.

Satpathy, A.T., Kc, W., Albring, J.C., Edelson, B.T., Kretzer, N.M., Bhattacharya, D., Murphy, T.L., and Murphy, K.M. (2012). Zbtb46 expression distinguishes classical dendritic cells and their committed progenitors from other immune lineages. J. Exp. Med. 209, 1135–1152.

Sauter, R.J., Sauter, M., Reis, E.S., Emschermann, F.N., Nording, H., Ebenhoch, S., Kraft, P., Munzer, P., Mauler, M., Rheinlaender, J., et al. (2018). Functional relevance of the anaphylatoxin receptor C3aR for platelet function and arterial thrombus formation marks an intersection point between innate immunity and thrombosis. Circulation 138, 1720–1735.

Soriano, P. (1999). Generalized lacZ expression with the ROSA26 Cre reporter strain. Nat. Genet. 21, 70–71.

Subramanian, A., Tamayo, P., Mootha, V.K., Mukherjee, S., Ebert, B.L., Gillette, M.A., Paulovich, A., Pomeroy, S.L., Golub, T.R., Lander, E.S., and Mesirov, J.P. (2005). Gene set enrichment analysis: a knowledge-based approach for interpreting genome-wide expression profiles. Proc. Natl. Acad. Sci. U S A 102, 15545–15550.

Tabas, I., and Lichtman, A.H. (2017). Monocyte-Macrophages and T Cells in atherosclerosis. Immunity 47, 621–634.

Tenger, C., and Zhou, X. (2003). Apolipoprotein E modulates immune activation by acting on the antigen-presenting cell. Immunology 109, 392–397.

Thunemann, M., Schorg, B.F., Feil, S., Lin, Y., Voelkl, J., Golla, M., Vachaviolos, A., Kohlhofer, U., Quintanilla-Martinez, L., Olbrich, M., et al. (2017). Cre/lox-assisted non-invasive in vivo tracking of specific cell populations by positron emission tomography. Nat. Commun. 8, 017–00482.

Tilstam, P.V., Gijbels, M.J., Habbeddine, M., Cudejko, C., Asare, Y., Theelen, W., Zhou, B., Doring, Y., Drechsler, M., Pawig, L., et al. (2014). Bone marrow-specific knock-in of a non-activatable Ikkalpha kinase mutant influences haematopoiesis but not atherosclerosis in Apoe-deficient mice. PLoS One 9, e87452.

Trusca, V.G., Fuior, E.V., Florea, I.C., Kardassis, D., Simionescu, M., and Gafencu, A.V. (2011). Macrophage-specific up-regulation of apolipoprotein E gene expression by STAT1 is achieved via long range genomic interactions. J. Biol. Chem. 286, 13891–13904.

Van Eck, M., De Winther, M.P., Herijgers, N., Havekes, L.M., Hofker, M.H., Groot, P.H., and Van Berkel, T.J. (2000). Effect of human scavenger receptor class A overexpression in bone marrow-derived cells on cholesterol levels and atherosclerosis in ApoE-deficient mice. Arterioscler Thromb.Vasc. Biol. 20, 2600–2606.

Wang, M., Subramanian, M., Abramowicz, S., Murphy, A.J., Gonen, A., Witztum, J., Welch, C., Tabas, I., Westerterp, M., and Tall, A.R. (2014). Interleukin-3/granulocyte macrophage colony-stimulating factor receptor promotes stem cell expansion, monocytosis, and atheroma macrophage burden in mice with hematopoietic ApoE deficiency. Arterioscler Thromb.Vasc. Biol. 34, 976–984.

Weisgraber, K.H., and Shinto, L.H. (1991). Identification of the disulfide-linked homodimer of apolipoprotein E3 in plasma.Impact on receptor binding activity. J. Biol. Chem. 266, 12029–12034.

Westerterp, M., Gautier, E.L., Ganda, A., Molusky, M.M., Wang, W., Fotakis, P., Wang, N., Randolph, G.J., D'agati, V.D., Yvan-Charvet, L., and Tall, A.R. (2017). Cholesterol accumulation in dendritic cells links the inflammasome to acquired immunity. Cell. Metab. 25, 1294–1304.

WHO (2019). World Health Organization cardiovascular disease risk charts: revised models to estimate risk in 21 global regions. Lancet Glob. Health 30, e1332–e1345. https://doi.org/10.1016/S2214-109X(19)30318-3.

Wolf, D., and Ley, K. (2019). Immunity and inflammation in atherosclerosis. Circ. Res. 124, 315–327.

Wolf, D., Zirlik, A., and Ley, K. (2015). Beyond vascular inflammation—recent advances in understanding atherosclerosis. Cell Mol. Life Sci. 72, 3853–3869.

Yilmaz, A., Lochno, M., Traeg, F., Cicha, I., Reiss, C., Stumpf, C., Raaz, D., Anger, T., Amann, K., Probst, T., et al. (2004). Emergence of dendritic cells in rupture-prone regions of vulnerable carotid plaques. Atherosclerosis 176, 101–110.

Zernecke, A. (2015). Dendritic cells in atherosclerosis. Arteriosclerosis Thromb.Vasc. Biol. 35, 763–770.

Zhang, S., Reddick, R., Piedrahita, J., and maeda, N. (1992). Spontaneous hypercholesterolemia and arterial lesions in mice lacking apolipoprotein E. Science 258, 468–471.

STAR★METHODS

KEY RESOURCES TABLE

REAGENT or RESOURCE	SOURCE	IDENTIFIER
Experimental models: Organisms/strains		
Albumin^cre+	Jackson Laboratory	Stock no. 003574; RRID: IMSR_JAX:003574
ApoE^-/-	Jackson Laboratory	Stock no. 002052; RRID: IMSR_JAX:002052
ApoE^fl/fl	Jackson Laboratory	Stock no. 028530; RRID: IMSR_JAX:028530
C57BL/6J	Jackson Laboratory	Stock no. 000664; RRID: IMSR_JAX:000664
CD11c.DTR-GFP	Jackson Laboratory	Stock no. 004509; RRID: IMSR_JAX:004509
CD11c^cre+	Jackson Laboratory	Stock no. 008068; RRID: IMSR_JAX:008068
LacZ^fl/fl	Jackson Laboratory	Stock no. 003474; RRID: IMSR_JAX:003474
Antibodies		
CD103 PerCP-Cy5.5 clone 2E7	Biolegend	Cat. no. 121416; RRID: AB_2128621
CD11b PE clone M1/70	Biolegend	Cat. no. 101208; RRID: AB_312791
CD11c APC clone N418	Biolegend	Cat. no. 117310; RRID:AB_313779
CD11c MicroBeads UltraPure, mouse	Miltenyi Biotec	Cat. no. 130-125-835
CD172a PE-Dazzle594 clone P84	Biolegend	Cat. no. 144015; RRID:AB_2565279
CD19 Brilliant Violet® 510 clone: 6D5	Biolegend	Cat. no. 115545; RRID:AB_2562136
CD45 PB clone: 30-F11	Biolegend	Cat. no. 103125; RRID:AB_493536
CD8a Brilliant Violet® 650 clone 53-6.7	Biolegend	Cat. no. 100741; RRID:AB_11124344
DT antibody IgG1 11D9	Abcam	Cat. no. ab53827; RRID:AB_879808
F4/80 PE/Cyanine7 clone QA17A29	Biolegend	Cat. no. 157307; RRID:AB_2832550
I-A/I-E MHCII FITC clone M5/114.15.2	Biolegend	Cat. no. 107605; RRID:AB_313320
Invitrogen®Goat anti-Mouse IgG	Thermo Scientific	Cat. no. 62-6540; RRID:AB_2533949
IRDye® 800CW Goat anti-Rabbit IgG	Li-Cor	Cat. no. 926-32211; RRID:AB_621843
Ly-6C Alexa Fluor® 700 clone 1A8	Biolegend	Cat. no. 127621; RRID:AB_10640452
Rabbit monoclonal to Apolipoprotein E	Abcam	Cat. no. ab183596; RRID:AB_2832971
TCR-b chain Brilliant Violet®510 clone H57-597	Biolegend	Cat. no. 109233; RRID:AB_2562349
Chemicals, peptides, and recombinant proteins		
4 x Laemmli sample buffer	Biorad	Cat. no. 1610747
acetylated LDL	Thermo Scientific	Cat. no. L35354
Acrylamide Rotiphorese® Gel 30	Carl Roth	Cat. no. 3029.1
APS	Carl Roth	Cat. no. 9592.3
Baytril® (Enrofloxacine 2,5% ad us. vet.)	Bayer	PZN P11004248
Bovine Serum albumin fraction V	Merck (Sigma Aldrich)	Cat. no. 10735094001
Chemiluminescent Peroxidase Substrate for ELISA	Merck (Sigma Aldrich)	Cat. no. CPS260
Collagenase I	Sigma Aldrich	Cat. no. C-0130
Collagenase XI	Sigma Aldrich	Cat. no. C-7657
Coomassie Brilliant Blue R-250 protein stain powder	Biorad	Cat. no. 1610400
Diphtheria toxin	Merck	Cat. no. D0564
Diphtheria toxin (mutant CRM197)	List Biological Laboratories	Cat. no. 149A
DNase 1,type 2	Sigma Aldrich	Cat. no. D-4527

Continued

REAGENT or RESOURCE	SOURCE	IDENTIFIER
DPBS	Gibco	Cat. no. 14190-144
EDTA, 0.5M, pH 8.0	Invitrogen	Cat. no. AM9260G
Eosine G 1% solution	Merck (Sigma Aldrich)	Cat. no. 117081
Ethidium bromide solution	Sigma Aldrich	Cat. no. E1510-10ML
Fetal bovine serum	Thermo Scientific	Cat. no. 26140-079
Formaldehyde solution 4%, buffered, pH 6.9	Merck	Cat. no. 1004960700
Glycine	Merck (Sigma Aldrich)	Cat. no. G8898-500G
HEPES buffer	Gibco	Cat. no. 11360-070
High cholesterol diet EF, 10mm, Paigen	Ssniff	Cat. no. S8127-E510
Hyaluronidase	Sigma Aldrich	Cat. no. H-3506
Invitrogen Agarose UltraPure™	Thermo Scientific	Cat. no. 16500500
Isoflurane	CP Pharma	Cat. no. 1214
Mayers Haemalaun	Merck (Sigma Aldrich)	Cat. no. 109249
Oil Red O C.I. 26125	Merck	Cat. no. 1052300025
OneComp compensation beads	BD	Cat. no. 552845
PBS without Ca and Mg	Gibco	Cat. no. 14190-169
Penicillin and streptomycin	Sigma Aldrich	Cat. no. P4333
RBC Lysis Buffer (eBioscience™)	Thermo Scientific	Cat. no. 00-4333-57
Recombinant mouse GMCSF protein	Peprotech	Cat. no. 415-ML-010/CF
ROTI® Histol	Roth	Cat. no. 6640
RPMI 1640 medium	Thermo Scientific	Cat. no. 11875-093
SDS blotting grade	Carl Roth	Cat. no. 0183.1
Skimmed milk powder	AppliChem	Cat. no. A0830
Streptavidin AP conjugate	Merck (Roche)	Cat. no. 11089161001
TEMED	Carl Roth	Cat. no. 2367.4
TRIS	Carl Roth	Cat. no. 4855.2
X-Gal	Merck (Sigma Aldrich)	Cat. no. 3117073001
Zombie NIR™Fixable Viability Kit, APC-Fire 750	Biolegend	Cat. no. 423105
β-Mercaptoethanol	Sigma Aldrich	Cat. no. M6250
Critical commercial assays		
Cholesterol Efflux Kit (cell based)	Abcam	Cat. no. ab196985
FastStart SYBR Green Master Mix	Roche	Cat. no. 4673492001
GoScript™ Reverse Transcriptase Kit	Promega	Cat. no. A5001
Mouse Apolipoprotein E ELISA Kit	Abcam	Cat. no. ab215086
Mouse IL-1 beta/IL-1F2 Quantikine ELISA Kit	R&D	Cat. no. MLB00C
MyTaq™ Extract-PCR Kit	meridian bioscience	Cat. no. BIO-21126
Proteome Profiler Array Kit	R&D	Cat. no. ARY003C
Qiagen RNeasy Mini Kit	Quiagen	Cat. no. 74104
Oligonucleotides		
mouse ApoE	eurofins	5'-ACAGATCAGCTCGAGTGGCAAA-3' (fw) 5'-ATCTTGCGCAGGTGTGTGGAGA-3' (rv)
mouse ATP binding cassette A1 (ABCA1)	eurofins	5'-AGTTTCGGTATGGCGGGTTT-3' (fw) 5'-AGCATGCCAGCCCTTGTTAT-3' (rv)

(Continued on next page)

Continued

REAGENT or RESOURCE	SOURCE	IDENTIFIER
mouse ATP binding cassette G1 (ABCG1)	eurofins	5'-ACCTACCACAACCCAGCAGACTTT-3' (fw) 5'-GGTGCCAAAGAAACGGGTTCACAT-3' (rv)
mouse liver x receptor (LXR)	eurofins	5'-CTCAATGCCTGATGTTTCTCCT-3' (fw) 5'-TCCAACCCTATCCCTAAAGCAA-3' (rv)
Primers for genotyping, see Table S1	Eurofins	N/A
Deposited data		
Gene array data	This paper	GEO: GSE191044
Software and algorithms		
AxioVision	Zeiss	https://www.micro-shop.zeiss.com/de/de/system/software+axiovision-axiovision+basissoftware-axiovision+software/10221/
Cellquest Pro	BD Biosciences	https://www.bd.com/de-de/products/biosciences
GraphPad Prism 9.2.0	GraphPad	https://www.graphpad.com/scientific-software/prism/
GSEA Software	Broad Institute	https://www.gsea-msigdb.org/gsea/index.jsp
ImageJ	Wayne Rasband, NIH	https://imagej.nih.gov/ij/
Kaluza Analysis 2.1	Beckman Coulter	https://www.beckman.de/flow-cytometry/software/kaluza
Software package R	The R foundation	https://www.r-project.org

RESOURCE AVAILABILITY

Lead contact

Requests for resources and reagents should be directed to and will be fulfilled by the lead contact, Harald F. Langer (harald.langer@uksh.de).

Materials availability

This study did not generate new unique reagents.

Data and code availability

- Gene array data have been deposited at the GEO database (record number GSE, 191044). All other data reported in this paper will be shared by the lead contact upon request.

- This paper does not report original code.

- Any additional information required to reanalyze the data reported in this paper is available from the lead contact upon request.

EXPERIMENTAL MODEL AND SUBJECT DETAILS

Mouse models

C57Bl/6J mice (WT), ApoE⁻/⁻ mice, CD11cᶜʳᵉ⁺ (expressing the Cre recombinase under the control of the CD11c promoter) mice, CD11c.DTR-GFP (transgenic mice that express the primate diphtheria toxin (DT) receptor (DTR) as well as green fluorescent protein (GFP) under control of the DC-specific CD11c promoter (Jung et al., 2002)) mice were initially obtained from the Jackson laboratory and were bred in our animal facilities. Mice carrying the ROSA26 LacZ Cre reporter (R26R) allele (Soriano, 1999) were generated on an ApoE-deficient/ C57BL/6J background by crossing the parental lines (Feil et al., 2014a). Albᶜʳᵉ⁺ mice (expressing the Cre recombinase under the control of the albumin promoter) were originally obtained from the Jackson laboratory and bred at our animal facilities. ApoEᶠˡ/ᶠˡ mice were obtained from the Jackson laboratory with permission of Dr. Theodore Mazzone. Mice were genotyped using primers obtained from

Eurofins and protocols obtained from Jackson Laboratories. The mice were kept in open cages in groups of at least two to a maximum of five animals. All mice had ad libitum access to food and water and were maintained in a specific-pathogen free facility with a 12h:12h light:dark cycle. After irradiation of 6 week old mice, they were put into individually ventilated cages (IVC). Mice were euthanized for tissue harvest by intracardial debleeding under deep isoflurane anaesthesia.

Both male and female mice at the age of 6 to 8 weeks were used in all our studies. All animal experiments were approved by governmental authorities and performed in accordance with the German law guidelines of animal care (approvals M03/10 and M16/15).

METHOD DETAILS

Isolation and cultivation of BM derived CD11c$^+$ cells

CD11c$^+$ cells derived from bone marrow (BM derived CD11c$^+$ cells) were generated according to the previously described procedure by Inaba et al.(Inaba et al., 1992) with some modifications: After isoflurane anaesthesia and neck fracture, the femurs and tibiae were removed, cleanly dissected from muscles and tendons and disinfected in ethanol (one to two minutes). After washing the bones twice in DC medium (RPMI-1640 complete medium supplemented with 10% FCS, 1mM HEPES, 50μM 2-ME, 100 U/mL penicillin (Gibco) and 100 μg/mL streptomycin (Gibco) and mGM-CSF (20 ng/mL)), the epiphyses were cut on both sides and the bone marrow was flushed with DC medium using a 27G cannula into a 50mL Falcon tube. Cells were then pipetted through a 70μm cell strainer into fresh tubes and pelleted at 250g for five minutes. This was followed by lysis of the erythrocytes using RBC lysis buffer. After another centrifugation, the supernatant was discarded and the cell pellet was resuspended in DC medium and divided into 3mL each in a 6-cavity plate. Cells were cultivated for 7 days and media was changed every other day with mGM-CSF being added freshly every time. For some experiments, acLDL (10μg/mL) was added to the media on day 6 and left on the cells for 24h.

Generation of CD11c reporter mice

ApoE$^{-/-}$ mice were bred to CD11c^{cre+} and LacZ$^{fl/fl}$ mice to obtain a mouse line, that was homozygous for ApoE$^{-/-}$, CD11c^{cre+} and LacZ$^{fl/fl}$. Cre$^-$ littermates were used as controls. LacZ$^{fl/fl}$ mice carry a loxP flanked neo cassette upstream of a β-galactosidase (LacZ) sequence. Removal of the neo cassette by cre recombination results in LacZ expression in cre-expressing tissues (Soriano, 1999).

Generation of cell-specific ApoE$^{-/-}$ mice

ApoE$^{fl/fl}$ mice were bred to CD11c^{cre+} or Alb^{cre+} mice to obtain mouse lines, that do not produce ApoE either in liver cells (Alb^{cre+}ApoE$^{fl/fl}$) or in CD11c$^+$ cells (CD11c^{cre+}ApoE$^{fl/fl}$).

LacZ staining

X-Gal Stock solution: 40mg/mL X-Gal in dimethylsulfoxide. 10mL were prepared and stored at 1mL aliquots at −20°C.

X-Gal staining solution: 2mM MgCl$_2$, 2.5mM K$_3$Fn(CN)$_6$, 2.5mM K$_4$Fn(CN)$_6$ in PBS pH 7.4. 500mL were prepared and stored in the dark at RT. Before use, X-Gal stock solution (40mg/mL) was added to a final concentration of 1mg/mL of X-Gal. Depending on the amount of tissue to be stained, 2 to 20mL of X-Gal staining solution per mouse were prepared.

X-Gal staining of whole-mount aortae or paraffin embedded sections of aortae was carried out as described (Feil et al., 2014b; Thunemann et al., 2017): Animals were transcardially perfused with Heparin-PBS (PBS with 250 mg/L heparin) followed by PBS containing 2% formaldehyde and 0.2% glutaraldehyde. Explanted aortae were fixed for 20 minutes in the same fixative solution at room temperature, washed twice with PBS for 5 minutes under gentle shaking and incubated overnight at room temperature in the dark under gentle shaking in X-Gal staining solution. After staining, aortae were again washed three times with PBS for 5 minutes under gentle shaking and stored at 4°C in 70% ethanol. Images for analysis were taken using a digital camera attached to a stereo microscope (Zeiss, Oberkochen, Germany). For paraffin embedded sections, aortae were dehydrated in increasing concentrations of ethanol (70%, 80% and 95%) 45 min each, followed by three times absolute ethanol, 1 h each. Tissue was cleared twice in Roti-Histol (for 30 min and for another 15 min) Aortae were immersed in paraffin 3 times for 1 h to overnight and

embedded in paraffin. The aorta was placed in a small mold in appropriate orientation for cross-sectioning and the paraffin block was sectioned at 6 μm thickness using a microtome. Then, the aortae were deparaffinised as follows: Roti-Histol (2 x for 3 min), 100% ethanol (2 x for 3 min), 95% ethanol (1 x for 3 min), 70% ethanol (1 x for 3 min). Then, slides were rinsed with cold tap water. X-Gal-stained paraffin sections were co-stained using a standard H and E staining protocol.

LacZ (blue) area and total surface area of explanted aortae were measured using ImageJ and calculated as a percentage of the ratio of LacZ/total surface area.

Generation of BM chimeras

The generation of BM chimeras was carried out as described previously with minor modifications (Tilstam et al., 2014): BM cells (5×10^6/mouse) from BM donor mice were flushed from the femur and tibia marrow cavities. The resulting cell suspension was subsequently administered to ApoE$^{-/-}$ recipient mice by retrobulbar injection one day after a lethal dose of whole-body irradiation (2×6.5 Gy. Time between irradiations was 4 hours) with a Gamma Irradiation unit (Gammacell GC40 Exactor from Nordion) Caesium-gamma irradiation source (Cs147). For two weeks after irradiation, mice were treated with antibiotics (Baytril®, 1mL/100mL drinking water). After three weeks of recovery, the mice were put on a high-cholesterol diet (Ssniff, S8127-E510, EF, 10mm, Paigen) for 6 weeks. Detection of chimerism was done by screening genomic DNA from blood of the recipients for the DTR receptor using PCR.

Oil red O staining

Oil Red O staining of aortae was carried out as described previously (Muller et al., 2013): After euthanasia of the animals, the vessels were perfused with saline *in situ* followed by perfusion with 4% paraformaldehyde through the left ventricle. Subsequently, the vessels were transferred into 4% PFA for fixation and left there for 24h. Arteries were then stained with Oil Red O using following protocol:

The vessels were washed in dH$_2$O for one to two minutes and then transferred to 50% ethanol for three minutes. The vessels were then stained for 25 to 30 minutes in the Oil Red O working solution (60mL stock solution - 0.5g oil red in 100mL 100% ethanol plus 40mL dH$_2$0), rinsed for one to two minutes in dH$_2$O and then stored again in 4% paraformaldehyde at 4°C until further preparation and microscopy. Arteries were cut open and pinned onto agarose gels. Afterwards, the vessels were photographed with a Zeiss Axiovert 200 and the Axiocam MRc5 (Zeiss) using the Axio Vision software. Plaque areas and the total vessel area were measured using Image J software and the relative plaque extension was expressed as percentage of the total vessel area.

Enzyme linked immunosorbent assay (ELISA)

An ELISA to determine the development of antibodies against diphtheria toxin (DT) after long time DT treatment was performed according to Buch et al. (Buch et al., 2005). For the assay, a 96-well plate was coated with 2μg/mL DT (mutant CRM197, List Biological Laboratories) at 4°C overnight and the free binding sites of the plate were blocked the following day with 0.5% BSA in PBS for two hours at RT. Subsequently, the sera (from retrobulbar blood) of the DT-treated chimeras (or control animals) were applied and incubated at 37°C for one hour. A monoclonal antibody against DT (IgG1 isotype; Abcam) served as a standard. After washing three times with 0.5% PBST, a biotinylated Goat anti Mouse IgG1 (Thermo Scientific) antibody was pipetted onto the plate at a concentration of 1μg/mL, incubated for one hour at RT and after washing three times, alkaline phosphatase coupled streptavidin (1:3000, Roche) was applied. IgG in the sera was then visualised using an alkaline phosphatase substrate solution (0.4mg/mL, Roche) and the optical density (OD) at 405nm versus 570nm was compared with the standard curve.

For detecting ApoE in sera of mice, a commercially available ELISA kit from Abcam (Berlin, Germany) was used and carried out according to the manufacturer's protocol. For the detection of IL-1β in sera of mice, a commercially available ELISA kit from R&D Systems (Minneapolis, USA) was used and carried out according to the manufacturer's protocol.

Proteome profiler

BM derived CD11c$^+$ cells (vehicle ctrl versus loaded with acLDL 10μg/mL for 24 hours) were analyzed for phosphorylated kinases by a membrane-based antibody array (Proteome Profiler Array Kit, ARY003C, R&D) following the manufacturers protocol.

Cholesterol efflux analysis

BM derived CD11c$^+$ cells (loaded with acLDL on day 6 with 10μg/mL for 24 hours or treated with vehicle control) were analyzed for their ability to perform cholesterol efflux using a cell-based cholesterol efflux kit by Abcam (ab196985) following the manufacturer's instructions. Murine WT serum was used as cholesterol acceptor.

Lipid analysis

Cholesterol, high-density (HDL), low-density (LDL) and very low-density (VLDL) cholesterol levels in the blood serum were measured using a homogeneous enzymatic assay on Synchron LX20 test system, Beckman-Coulter with IFCC-standardised methods. Measurement of triglycerides was performed with a standardised clinical chemistry assay on a Synchron LX20 test system, Beckman-Coulter (triglyceride GPO reagent after lipase pre-treatment).

Flow cytometry

For analysis of aortic cells, the organs were carefully dissected under the dissection microscope (adventitiae from aortas should be kept). Organs were incubated with 20-30 mL of PBS containing 2% of heparin. Aortae were cut into small pieces and digested in 2.5–5 mL of enzyme cocktail, containing 450 U/mL collagenase type I, 250 U/mL collagenase type XI, 120 U/mL hyaluronidase type I-s, 120 U/mL DNAse 1 in 1x HBSS(with Ca and Mg). Samples were incubated in an Eppendorf ThermoMixer®C at 37°C for 50-60 min (150rpm). After incubation, samples were pipetted several times up and down to break pieces of aorta. Suspensions were filtered through 70 μm cell strainers. Rest of the aorta's pieces were smashed through 70 μm cell strainer, cell suspensions were collected. Samples were centrifuged at 250g for 5 min, 4°C. Supernatant was discarded. Samples were re-suspended using FACS buffer (PBS without Ca and Mg (Gibco, cat. no. 14190169), 1% FCS, 0.09% NaAc, 2mM EDTA) and the cell number was counted under the microscope.

For analysis of spleen cells, organs were collected and put in a petri dish containing PBS. Spleens were cut with surgical scissors and mashed with the help of the plunger of a sterile syringe. Samples were pipetted and pressed trough a 40μm cell filter into a 50mL falcon tube, then filled up with PBS to 10mL. Samples were centrifuged at 250g for 5 minutes, supernatant was discarded. Red blood cell lysis was performed by re-suspending pellet in 5mL ice-cold RBC lysis buffer for 5 minutes on ice. 5mL RPMI + FBS were added to stop RBC lysis and samples were centrifuged again at 250g for 5 minutes. Supernatant was discarded and pellet re-suspended in 5mL FACS buffer. Then, samples were put through 70μm cell strainers into new 50mL falcon tubes.

For FACS analysis of whole blood, blood of deeply isoflurane-anesthetized mice was collected through heart puncture into Eppendorf vials with EDTA. A dilution of EDTA anticoagulated blood:FACS buffer 1:4 was made. Antibodies could then be directly added to diluted whole blood. Further procedure was performed in analogy to FACS analysis of spleens, lymph nodes and aortae.

Cells were stained with antibodies Anti-I-A/I-E MHCII anti mouse [clone: M5/114.15.2] FITC; Anti CD103 anti mouse Antibody [clone: 2E7], PerCP/Cy5.5; Anti mouse/human CD11b [clone M1/70], PE; Anti CD172a anti mouse [clone: P84], PE-TR/PE-Dazzle594; Anti-mouse F4/80 Recombinant Antibody [clone QA17A29], PE/Cyanine7; Anti mouse CD11c [clone N418], APC; Anti-Ly-6C (Alexa Fluor® 700); Zombie NIR™ Fixable Viability Kit, APC-Fire 750; Anti CD45 anti mouse (PB (Pacific Blue)) [clone: 30-F11], BV421; Anti-TCR-b chain Armenian Hamster Monoclonal Antibody (Brilliant Violet® 510) [clone: H57-597]; Anti CD19 anti mouse (Brilliant Violet® 510) [clone: 6D5]; Anti CD8a anti mouse (Brilliant Violet® 650) [clone: 53-6.7] for 30 minutes on ice in the dark. After washing with FACS buffer, cells were fixed in 1% PFA for 15 minutes on ice and washed again afterwards. Unstained cells and cells treated with unspecific IgG antibodies served as controls. Analysis of single cell suspensions was carried out on a FACSCalibur (BD Biosciences) using Cellquest Pro Software and a Cytoflex S 4-laser cytometer (Beckman Coulter, Brea, CA, USA) using Kaluza Analysis 2.1 software (Beckman Coulter). Specific monoclonal antibody binding was expressed as the geometric mean fluorescence intensity (MFI).

Quantitative PCR

Cultivated BM derived CD11c$^+$ cells were rinsed with DC medium into a 50mL Falcon tube and pelleted at 250g for five minutes. The supernatant was aspirated and mRNA was isolated from the cell pellet using the

Qiagen RNeasy Mini Kit according to the manufacturer's instructions. After DNAse digestion, the obtained mRNA was transcribed into cDNA using the Promega kit. The genes to be analyzed were detected using specific primers and SYBR-Green Master Mix in the Roche LightCycler 480. Analysis was carried out with the help of the associated software via the Ct values.

Gene arrays

CD11c$^+$ cells were isolated from mouse spleens explanted from WT mice fed with standard diet (normal chow, NC), WT mice fed with high cholesterol diet (HC), ApoE$^{-/-}$ mice fed with NC and ApoE$^{-/-}$ mice fed with HC using CD11c MicroBeads UltraPure, MS Columns and a MiniMACS™ Separator (Miltenyi Biotec, USA). For each condition, RNA was isolated using columns including a DNAse-step followed by reverse transcription (all reagents from Qiagen, Valencia, CA). RNA was labelled and hybridized to Illumina MouseWG-6 v.2.0 Expression Bead Chips (Illumina, San Diego, USA) according to the manufacturer's instructions at the Genomics and Proteomics Core Facility of the German Cancer Research Centre, Heidelberg. For each sample, RNA was hybridized to a separate gene array.

Local pooled error test

For statistical analysis, the open source statistical software package R (www.r-project.org) was used including the local pooled error (LPE) test for differential expression discovery between two conditions (Jain et al., 2003). Gene chip data were analyzed as described previously (Cho et al., 2007). Non-expressed genes were excluded, followed by normalization of data and log2 transformation to achieve normal distribution. A false discovery rate (FDR) to discover probe sets differentially expressed with FDR <0.25 was used (Jain et al., 2005). Heat maps were constructed using R in a way that allows all conditions and genes to freely cluster both in the x- (condition) and y-axes (gene).

Gene set enrichment analysis

Gene set enrichment was analyzed using an open access software for gene set enrichment analysis (GSEA) (Subramanian et al., 2005). GSEA calculates an enrichment score, which indicates the degree of overrepresentation of gene sets and estimates its significance with adjustment for multiple hypothesis testing. As GSEA is of exploratory nature and has been designed to generate hypotheses, a false discovery rate of 0.25 was used. Due to the lack of coherence in most expression datasets, a more stringent FDR cut-off may lead to exclusion of potentially relevant results.

Western Blot

For generation of whole cell lysates, cells were lysed in RIPA buffer (150 mM NaCl, 50 mM TRIS, 0.1% SDS, 0.5% sodium deoxycholate, 1% Triton-X 100 and complete protease inhibitor cocktail and boiled in 4 x Laemmli SDS sample buffer (Bio Rad) for 10 min at 95°C. For analysis of sera from BM chimeras, 2μL serum was mixed with RIPA buffer and 4 x Laemmli SDS sample buffer to a total volume of 20 mL and boiled as described for whole cell lysates.

Next, samples were separated by SDS-polyacrylamide gel electrophoresis on 10% polyacrylamide gels and subjected to western blot analysis as described before (Langer et al., 2012; Sauter et al., 2018): After blotting, membranes were blocked with 5% skim milk in Tris-buffered saline 0.05% Tween-20 and incubated with primary antibody (Rabbit anti mouse ApoE from Abcam, ab183596) at 4°C overnight. Secondary antibody (anti rabbit from LI-COR, Bad Homburg, Germany, diluted 1:15000) was subsequently incubated for 1 hour at room temperature and membranes were washed thrice with Tris-buffered saline 0.05% Tween-20. Membranes were scanned with the Odyssey Infrared Imaging System (LI-COR, Bad Homburg, Germany) and analyzed.

After immunodetection, the membrane was washed twice with PBST and then stained with 0.1% Coomassie R-250 (Biorad) in methanol/water, 1:1, for 1 min, destained for 20 min in acetic acid/ethanol/water, 1:5:4, washed with water and air-dried.

QUANTIFICATION AND STATISTICAL ANALYSIS

Data are provided as means ± SD; n represents the number of experiments. Statistical analyses were carried out using GraphPad Prism version 9.2.0 software. Two-tailed Student's t-test was used to determine the statistical significance between two samples originated from the same population. Statistical

significance between more than two samples was determined by one-way ANOVA or two-way ANOVA with Bonferroni's post hoc test and a statistical threshold of p ≤ 0.05. Microarray Data were analyzed with GSEA software: The false discovery rate (FDR) is the estimated probability that a gene set with a given normalized enrichment score represents a false positive finding. The GSEA analysis report highlights enrichment gene sets with an FDR of less than 25% as those most likely to generate interesting hypotheses and drive further research, but provides analysis results for all analyzed gene sets. In general, given the lack of coherence in most expression datasets and the relatively small number of gene sets being analyzed, an FDR cut-off of 25% is appropriate (Subramanian et al., 2005).

ADDITIONAL RESOURCES

Not applicable.